Chemosphere 247 (2020) 125861

Contents lists available at ScienceDirect

Chemosphere

journal homepage: www.elsevier.com/locate/chemosphere

Characteristics and sources of $PM_{2.5}$ with focus on two severe pollution events in a coastal city of Qingdao, China

Yang Gao [a, b, 1, *], Huayao Shan [a, 1], Shaoqing Zhang [c, d, e, f], Lifang Sheng [f, g], Jianping Li [c, d], Junxi Zhang [h], Mingchen Ma [a], He Meng [i], Kun Luo [h], Huiwang Gao [a, b], Xiaohong Yao [a, b, **]

[a] Key Laboratory of Marine Environment and Ecology, Ministry of Education/Institute for Advanced Ocean Study, Ocean University of China, Qingdao, 266100, China
[b] Laboratory for Marine Ecology and Environmental Science, Qingdao National Laboratory for Marine Science and Technology, Qingdao, 266237, China
[c] Qingdao National Laboratory for Marine Science and Technology, Qingdao, 266237, China
[d] Key Laboratory of Physical Oceanography, Ministry of Education/Institute for Advanced Ocean Study/Frontiers Science Center for Deep Ocean Multispheres and Earth System (DOMES), Ocean University of China, Qingdao, 266100, China
[e] International Laboratory for High-Resolution Earth System Prediction (iHESP), Qingdao, 266237, China
[f] College of Oceanic and Atmospheric Sciences, Ocean University of China, Qingdao, 266100, China
[g] Ocean-Atmosphere Interaction and Climate Laboratory, Key Laboratory of Physical Oceanography, Ocean University of China, Qingdao, 266100, China
[h] State Key Laboratory of Clean Energy, Department of Energy Engineering, Zhejiang University, Hangzhou, Zhejiang, 310027, China
[i] Qingdao Environmental Monitoring Station, Qingdao, 266003, China

HIGHLIGHTS

- The local emission in Qingdao only contributed on average of one fourth during winter 2015.
- The transport plays a major role in modulating the air pollution in Qingdao.
- The sources of PM2.5 in Qingdao may vary dramatically in a short period of time.

ARTICLE INFO

Article history:
Received 6 November 2019
Received in revised form
31 December 2019
Accepted 6 January 2020
Available online 7 January 2020

Handling Editor: Xinlei Ge

Keywords:
$PM_{2.5}$
WRF
CMAQ
FLEXPART
Air parcel trajectories

ABSTRACT

In this study, the seasonal mean $PM_{2.5}$ concentration in Qingdao, a coastal city, during 2014–2018 was first analyzed and the winter, in particular of 2015, showed the highest concentration. To elucidate the sources and control factors of $PM_{2.5}$, three dimensional model Weather Research and Forecasting (WRF), Community Multiscale Air Quality model (CMAQ), as well as Flexible Particle model (FLEXPART), were used. During December 2015 and January 2016, modeling results showed that the mean contribution to $PM_{2.5}$ mass concentrations from local emissions in Qingdao was 25%, and the transport from north and west accounted for almost half. Over the two episodically polluted periods (29–31 December 2015; 15–17 January 2016), the local emissions in Qingdao surprisingly contributed to only 18% and 24% to $PM_{2.5}$ mass concentrations, respectively, indicating the dominant contributions from other regions, such as areas outside Qingdao in Shandong and Beijing-Tianjin-Hebei (BTH). The results show the sources region and contribution may vary remarkably along with the change in the pathways of the air parcel, inferred by the FLEXPART, while the near-surface $PM_{2.5}$ enhancement is largely caused by downward vertical advection and enhanced aerosol chemistry reactions, accompanied by simultaneous drop in the boundary layer height. This study also reveals that the transport contribution is sensitive to the air parcel trajectories. We, therefore, recommend the efficient emission control based on transport trajectories in short-term air quality improvement in Qingdao.

* Corresponding author. Key Laboratory of Marine Environment and Ecology, Ministry of Education/Institute for Advanced Ocean Study, Ocean University of China, Qingdao, 266100, China.
** Corresponding author. Key Laboratory of Marine Environment and Ecology, Ministry of Education/Institute for Advanced Ocean Study, Ocean University of China, Qingdao, 266100, China.
E-mail addresses: yanggao@ouc.edu.cn (Y. Gao), xhyao@ouc.edu.cn (X. Yao).
[1] Authors contribute equally to this study.

https://doi.org/10.1016/j.chemosphere.2020.125861
0045-6535/

1. Introduction

In recent years, China has experienced rapid economic development and urbanization, resulting in excessive emissions released into the atmosphere (Chan and Yao, 2008). The northern China is the area which was often invaded by severe haze pollution with high fine particulate matter ($PM_{2.5}$) concentrations (Ji et al., 2014; An et al., 2019; Duan et al., 2019). A number of studies have focused on the investigation of $PM_{2.5}$ pollution in North China Plain (Sun et al., 2016; Zhang et al., 2016; Du et al., 2019; Miao et al., 2019), in particular of the so-called "2 + 26" cities in Beijing-Tianjin-Hebei and surrounding regions (Wang et al., 2019). The studies in coastal areas are, however, limited, although more and more population is migrating from inland to coastal areas. For example, Qingdao is a coastal city located in Shandong Peninsula of eastern China and has the population of 9.4 million in 2018 with an increase of $1.0*10^5$ population per year (Qingdao statistical Yearbook, 2018; https://chinabookshop.net/shop?olsPage=products). It has been reported that Qingdao also suffers from the public human health problem associated with air pollution (Huang et al., 2018). In addition, the air pollutants therein are also more likely to affect the marine environment through the transport and deposition and play crucial roles in modulating the marine primary production (Zhang et al., 2019b). Therefore, it is vital to characterize the $PM_{2.5}$ in Qingdao, analyze $PM_{2.5}$ sources and reveal mechanisms in increasing $PM_{2.5}$ concentrations in particular during the severe pollution events.

Qingdao is featured by the heating season in winter, similar as other inland northern cities such as Beijing, but clean marine environment in summer, which may therefore face large winter and summer particle ratio in contrast to the southern coastal cities. For instance, in terms of the total carbon (the summation of organic carbon and element carbon), the ratio of winter to summer in Qingdao is 5.1, much higher than the southern coastal cities such as Shanghai (2.3), Xiamen (3.5), Guangzhou (4.0) and Hong Kong (1.6) in 2003 (Cao et al., 2007). More emissions and worse dispersion conditions determined that severe $PM_{2.5}$ pollution events occurred mainly in winter rather than other seasons (Gao et al., 2011; Zhang et al., 2019c).

$PM_{2.5}$ pollution is often attributed to both the modulation of meteorology and emissions. For example, by comparing the two same month of December in two adjacent years (2014 vs. 2015), Chang et al. (2016) concluded that $PM_{2.5}$ pollution in December 2015 was likely caused by the enhanced southeasterly wind and decreased wind speed in China. Similar comparison was also conducted in Liu et al. (2017), showing that lower planetary boundary layer height (PBLH) and higher relative humidity was found in December 2015 relative to 2014 in Beijing-Tianjin-Hebei areas. Moreover, Zhang et al. (2019a) further investigated the mechanism, and found that a seesaw pattern of high $PM_{2.5}$ in December and relatively low $PM_{2.5}$ concentration in January 2016 over the North China Plain, mainly attributable to the changes of Arctic Oscillation (AO) which induced the sub-seasonal variations. Similarly, during December 2015, Qingdao experienced severe haze pollution events (Li et al., 2017; Zhang et al., 2019d), and the underlying mechanism and sources of $PM_{2.5}$ in Qingdao are still unclear, which is one of the major targets of this study.

In what follows, the seasonal variations in $PM_{2.5}$ mass concentration during the past five years in Qingdao were first characterized, followed by the model evaluation of $PM_{2.5}$ and the associated inorganic species. At the end, the three dimensional models of WRF/CMAQ, CMAQ-ISAM and WRF/FLEXPART were utilized to elucidate the governing processes and sources of $PM_{2.5}$.

2. Methods and model configurations

The observational data such as $PM_{2.5}$, SO_2 and NO_2 were downloaded from http://www.pm25.in (last access: 15 December 2018). The inorganic aerosol ions such as SO_4^{2-}, NO_3^- and NH_4^+ in $PM_{2.5}$ as well as NH_3, SO_2, HNO_3 and HNO_2 gases were measured hourly by the URG-9000D Ambient Ion Monitor-Ion Chromatograph (AIM-IC) during 18 November 2015 to 11 January 2016 on the second floor of an academic building in the campus of Ocean University of China (OUC; 36.16°N, 120.50°E), located at the semi-urban area of Qingdao. More details about the measurement method can be found in Teng et al. (2017).

Three dimensional Weather Research and Forecasting (WRF) model version 3.8.1 (Skamarock et al., 2008) was used to produce the meteorological data, which can be further used as input for both the Eulerian model Community Multiscale Air Quality model (CMAQ) version 5.2 (Byun and Schere, 2006) and lagrangian model Flexible Particle model (FLEXPART) version 3.1 (Brioude et al., 2013). For source-receptor, CMAQ Integrated Source Apportionment Method (CMAQ-ISAM) 5.0.2 was used. WRF/CMAQ has been widely used in previous studies (Gao et al., 2013; Wong et al., 2015; Zhang et al., 2019a). The setting of WRF/CMAQ is the same as documented by Zhang et al. (2019a) and Ma et al. (2019). FLEXPART was mainly used to forward or backward illuminate the transport and diffusion of atmospheric pollutants by tracking the tracers of particles released from sources. The process analysis (PA) is a module embedded in CMAQ which can calculate the contributions of physical and chemical processes to various of species. For the particulate matters, the Integrated Process Rate (IPR) was available to investigate contributions of nine individual processes, including horizontal advection (HADV), horizontal diffusion (HDIF), vertical advection (ZADV), vertical diffusion (VDIF), gas phase chemistry (CHEM), dry deposition (DDEP), cloud processes (CLDS), aerosol processes (AERO) and emission (EMIS).

3. Characteristics of $PM_{2.5}$ measured in Qingdao

Seasonal mean $PM_{2.5}$ concentrations in each year from 2014 to 2018 at the nine stations are shown in Fig. 1, with mean and standard deviation shown in Table S1 in the supporting information. The mean $PM_{2.5}$ concentration in winter over the nine stations in Qingdao is 67 ± 13 μg/m^3, substantially higher than the mean values of 45 ± 10 μg/m^3 in spring, 28 ± 9 μg/m^3 in summer and 38 ± 10 μg/m^3 in fall, respectively. The nine stations in Qingdao show a general decrease of $PM_{2.5}$ from 2014 to 2018 in spring, summer and fall (Fig. 1a,b,c), and in winter, the $PM_{2.5}$ concentration in the year of 2015 (blue line and dots in Fig. 1d) is strikingly higher than any other single year for all the stations. The detailed mechanism will be discussed in the latter sections. In terms of the spatial heterogeneity, by comparing different stations for a specific season and year, the variations are in general not too large, with relatively lower value (five-year mean of 36 ± 14 μg/m^3) in the rural area of Yangkou (north of Qingdao, location shown in Fig. S1b in the supporting information), followed by the coastal sites including Shinan-E (five-year mean of 38 ± 14 μg/m^3) and Shinan-W (five-year mean of 39 ± 17 μg/m^3), whereas the five-year mean in the other six stations ranges from 44 ± 17 μg/m^3 to 51 ± 20 μg/m^3, with the highest value in Licang where industry is relatively dense. Note that the so-called West Coast New Area of Qingdao (named Huangdao in Fig. 1), officially developed in 2014 and connected with the urban areas of Qingdao through the harbor tunnel and cross-sea bridge, ranks indeed the second polluted area, based on the five-year mean concentration (50 ± 21 μg/m^3), among the nine

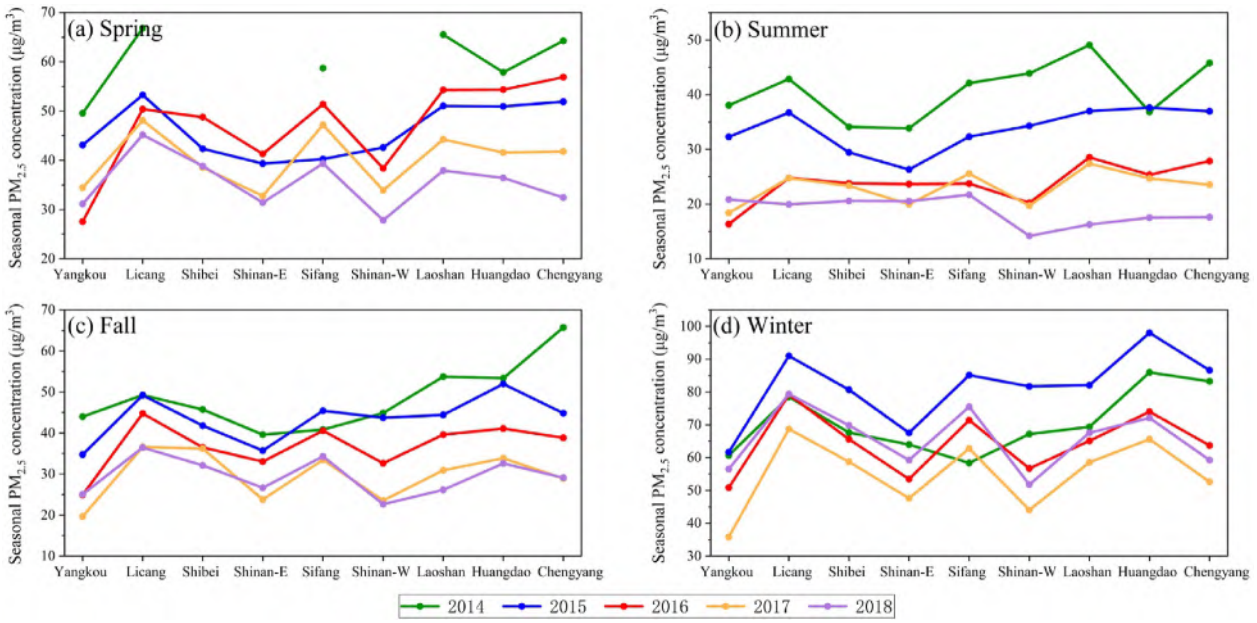

Fig. 1. Seasonal mean $PM_{2.5}$ variations at nine stations of Qingdao. The location of the stations is shown in Fig. S1b in the supporting information.

stations, posing air pollution challenges for this newly developed area.

The $PM_{2.5}$ concentrations in 2014–2018 are further compared with previous studies in order to argue the long-term variation in $PM_{2.5}$ in Qingdao. By conducting measurement at selected months in spring, autumn and winter, the mean value during 2011–2012 was found to be 102 ± 37 μg/m^3 in Licang and Shinan (Xu et al., 2015). These two sites correspond approximately to the site of Licang and Shinan-W in this study, showing mean value of 51 ± 18 μg/m^3 for the same three-season during 2014–2018 (Fig. 1; values can also be retrieved from Table S1), implicative of an obvious decrease associated with more stringent mitigation of air pollutants in the North China Plain including Qingdao. At the semi-urban site of OUC, the mean $PM_{2.5}$ concentration was reported as 135 μg/m^3 in winter 2003 (two-week measurement (Cao et al., 2012);) and 110 μg/m^3 during the winter of 2006–2007 (Wu et al., 2017). In contrast, the mean seasonal $PM_{2.5}$ ranges from 59 ± 40 μg/m^3 to 82 ± 59 μg/m^3 during 2014–2018 in the corresponding site (Laoshan), indicating a concentration drop as well. Nevertheless, severe $PM_{2.5}$ pollution events in Qingdao still occurred sometimes during 2014–2018, i.e., taking the urban site of Laoshan as an example, the maximal daily mean $PM_{2.5}$ of 326 μg/m^3, with 26 days exceeding 150 μg/m^3.

In addition to the total $PM_{2.5}$ mass concentrations, their inorganic aerosol ions including SO_4^{2-}, NO_3^- and NH_4^+ were also characterized and compared with previous observations in literature. The measurement results at the campus of OUC from 1 December 2015 to 11 January 2016 show mean concentrations of 12 ± 10, 16 ± 13, 10 ± 8 μg/m^3 for SO_4^{2-}, NO_3^- and NH_4^+, respectively, dominated by NO_3^-. In contrast, at the same location, the mean concentration for these three species is 21 ± 8 μg/m^3, 19 ± 9 μg/m^3 and 15 ± 5 μg/m^3 during an earlier measurement on 6–20 January 2003 (Cao et al., 2012), with dominant species of SO_4^{2-}. The SO_4^{2-} domination is also clearly visible at two other sites of Qingdao and nine other coastal cities in China (Table S2 from Wu et al. (2017)) during 1997–2010. Together, it is implicative of the efficient control of SO_2 recently as well as the increase of vehicles, making a shift in the dominant inorganic aerosol from SO_4^{2-} to NO_3^- (Tian et al., 2019; Xu et al., 2019).

4. Modeling analysis of severe $PM_{2.5}$ pollution events in Qingdao

4.1. Model evaluation of $PM_{2.5}$ and the inorganic aerosols against measurements

Since the abnormally high $PM_{2.5}$ occurred in the winter of 2015, mainly over December 2015 and January 2016, the three dimensional model WRF-CMAQ thereby focused on investigating possible processes governing the accumulation of severe $PM_{2.5}$ pollution during December 2015 and January 2016.

First, the model evaluation was performed. The time series of daily mean concentration of simulated and observed $PM_{2.5}$ as well as the inorganic species including NO^{3-}, SO_4^{2-} and NH_4^+ is shown in Fig. 2. The statistical metrics, including Normalized Mean Bias (NMB), Normalized Mean Error (NME), Mean Fractional Bias (MFB), Mean Fractional Error (MFE) and correlation coefficient (R) are shown in Table 1, with equations for these metrics shown in the

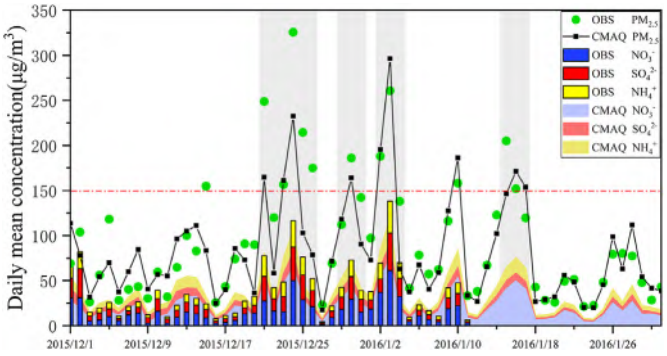

Fig. 2. Time series of daily mean concentration of simulated and observed $PM_{2.5}$ as well as the inorganic species including NO_3^-, SO_4^{2-} and NH_4^+. For the inorganic species, the histograms indicate the observations, whereas the shading areas indicate simulated results from CMAQ. For $PM_{2.5}$, the solid black line, with black squares marked in the corresponding date, represents the simulated values while the observed values were denoted by the green dots. The dashed red line indicates the value of 150 μg/m^3, whereas the gray shading marks the four episodic events.

Table 1
Statistics of simulated and observed $PM_{2.5}$ as well as the inorganic species in Qingdao.

	$PM_{2.5}$	NO_3^-	SO_4^{2-}	NH_4^+
NMB	−10%	41%	−41%	−5%
NME	26%	57%	46%	32%
MFB	−7%	43%	−31%	3%
MFE	26%	57%	46%	35%
R	0.85	0.83	0.82	0.83

supporting information. Based on air quality index (AQI) (HJ 633-2012), severe pollution (level V) was defined as daily mean $PM_{2.5}$ exceeding 150 μg/m^3, marked in red dashed line in Fig. 2. The events with mean concentration reaching or exceeding the threshold was shaded in gray, including four events during 21–26 December, 29–31 December, 2–4 January, and 15–17 January. The criteria for MFB and MFE was commonly selected as 50% and 75% (US-EPA, 2007), and the MFB/MFE values in Table 1 satisfied the criteria.

Based on Fig. 2, the observational mean $PM_{2.5}$ concentration over the two-month period was 92 μg/m^3, whereas the model mean was 83 μg/m^3, with mean bias of −9 μg/m^3, less than 10%. The inorganic aerosol of SO_4^{2-}, NO_3^- and NH_4^+ from the model accounted for 9%, 26% and 10%, respectively, with a total contribution of 45%, albeit of slightly higher, in general comparable to the observed value of 37%. During these four episodic events shaded in gray, the mean observed and simulated $PM_{2.5}$ concentrations were 183 μg/m^3 and 147 μg/m^3, respectively, with mean model bias of 20%. Over the first-three events (observed ions missing in the fourth event), the contribution of observed inorganic aerosol including SO_4^{2-} (12%), NO_3^- (15%), NH_4^+ (10%) to $PM_{2.5}$ is 37%, whereas the model well reproduced the contribution of 44%, with SO_4^{2-}, NO_3^- and NH_4^+ of 7%, 27% and 10%, respectively. The model in general meets the benchmark criteria, with high correlation of greater than 0.82 for both $PM_{2.5}$ and the associated inorganic species (Table 1).

The elucidation of the mechanism in particular of the sources and governing processes during these severe events may help to provide efficient control strategies. In the recent studies (Zhang et al., 2017, 2019d), they focused on two of the events (21–26 December and 2–4 January). One of the major findings is the transport from other regions plays a vital role (i.e., Fig. 5 in Zhang et al. (2019d)) in particular during the pollution period, i.e., more than half was contributed by the northern and southern regions of Qingdao (i.e., 16–22 December 2015; 1-6 Januanry, 2016). However, on the one hand, the region selections spanning a few provinces may not facilitate the actual control policies. To overcome this issue, we designed nine regions, which carefully considered the adjacent provinces and regions, as well as further areas; On the other hand, the zero out brute force method used in Zhang et al. (2019d) may not reflect the non-linearity resulting from complete emission shutting down, whereas the method of CMAQ-ISAM is designed in account of the nonlinearity in particular of the NOx chemistry and the subsequently nitrate formation (Kwok et al., 2013). Thus, we combine the ISAM with CMAQ, as well as the tool of process analysis, to elucidate the sources and main processes modulating the severe events.

4.2. The governing processes and source apportionment of $PM_{2.5}$ in Qingdao

During December 2015 and January 2016, there is a total of four major $PM_{2.5}$ episodic events, with two events partly investigated by Zhang et al. (2019d). We focus on the other events occurring on 29–31 December (Event I) and 15–17 January (Event II) to further explore the causes of heavy $PM_{2.5}$ pollution based on the combination of WRF/CMAQ, CMAQ-ISAM and WRF/FLEXPART. The contributions of different processes to near surface $PM_{2.5}$ are shown in Fig. 3a and b, with vertical profile of processes (within 1.5 km) shown in Fig. 3c and d. Note that the red line in Fig. 3a and b indicates the accumulated hourly change of $PM_{2.5}$, and the raw $PM_{2.5}$ concentration for each hour is the accumulated hourly change plus the base value at the starting hour (i.e., hour 00 on 29 December, 2015 in Fig. 3a). In other words, the variation of the red line is able to reflect the $PM_{2.5}$ fluctuation, albeit of smaller value due to the setting of starting value at 0 instead of the specific $PM_{2.5}$ hourly concentration.

In Event I (29–31 December 2015), the base $PM_{2.5}$ concentration, at the hour of 00:00 on 29 December 2015, was 132 μg/m^3. The peak period, with the higher $PM_{2.5}$ concentrations, during Event I is from 06:00 on 30 December to 00:00 on 31 December (black square in Fig. 3a), showing the mean $PM_{2.5}$ concentration of 177 μg/m^3. During the peak period, a fast increase in $PM_{2.5}$ concentrations is accompanied by a simultaneous drop in PBLH in the initial few hours, with mean PBLH of 468 m and the lowest value of only 100 m or so. The near-surface $PM_{2.5}$ enhancement is largely caused by downward vertical advection, enhanced aerosol chemistry reactions due to increasing reactants' concentrations, with the positive vertical advection within the PBL corresponding to the negative vertical advection above the PBL (ZADV yellow bar Fig. 3c). The downward vertical advection is more obvious if the vertical profile of processes (results not shown) was drawn during the peak period (06:00–12:00 on 30 December 2015), indicated by the red line in Fig. 3a. It thereby illustrates that along the reduction of boundary layer height, air pollutants from the upper layer (i.e., above the PBL height) were transmitted to the ground and enhancing aerosol reactions (pink color, denoted as AERO, in Fig. 3c). Similarly, enhanced ozone concentration resulting from vertical mixing was also found by Khiem et al. (2010) for ground ozone concentration in the Kanto region of Japan; Zhang et al. (2017) found that $PM_{2.5}$ in Qingdao is derived from the long-range transport at a high altitude, and then vertically transmitted to the near ground, resulting in an increase in $PM_{2.5}$ concentration near ground from 1 to 7 January 2016.

In Event II, the base $PM_{2.5}$ concentration, at 00:00 on 15 January 2016, was 107 μg/m^3. Through the peak $PM_{2.5}$ period from 23:00 on 16 January to 10:00 on 17 January 2016 (black square in Fig. 3b), the mean $PM_{2.5}$ concentration was 258 μg/m^3. In comparison to Event I, the PBLH in Event II is even lower (Fig. 3b), resulting in even severer $PM_{2.5}$ pollution. The processes of vertical advection (ZADV) and aerosol chemistry (AERO), etc., promoted the increase in mass concentration of ground-level $PM_{2.5}$ (Fig. 3d), which is similar to the Event I discussed above.

To further elucidate the transport contribution to high $PM_{2.5}$ concentrations in Qingdao, CMAQ-ISAM is used to quantify the contributions of air pollutants from different regions. The air pollutants emitted by different regions can be thereby marked. After entering the chemical transport mode of CMAQ, these pollutants will go through a series of chemical and physical processes, during which ISAM can continuously update the tags and closely track the sources of various pollutants.

When CMAQ-ISAM is applied to track the sources of $PM_{2.5}$ in Qingdao, nine emission source regions are tagged, shown in Fig. 4, namely Qingdao (QD), Shandong except Qingdao (SD), Beijing-Tianjin-Hebei (BTH), Jiangsu (JS), Anhui (AH), Henan (HN), other regions in Northern China (NC), Southern China (SC) and Western China (WC). In addition to the designated regions, ISAM automatically marks pollutants from the initial field (ICON), the boundary field (BCON) and other regions (OTHR). Due to the complex sources and compositions of $PM_{2.5}$, multiple species except secondary

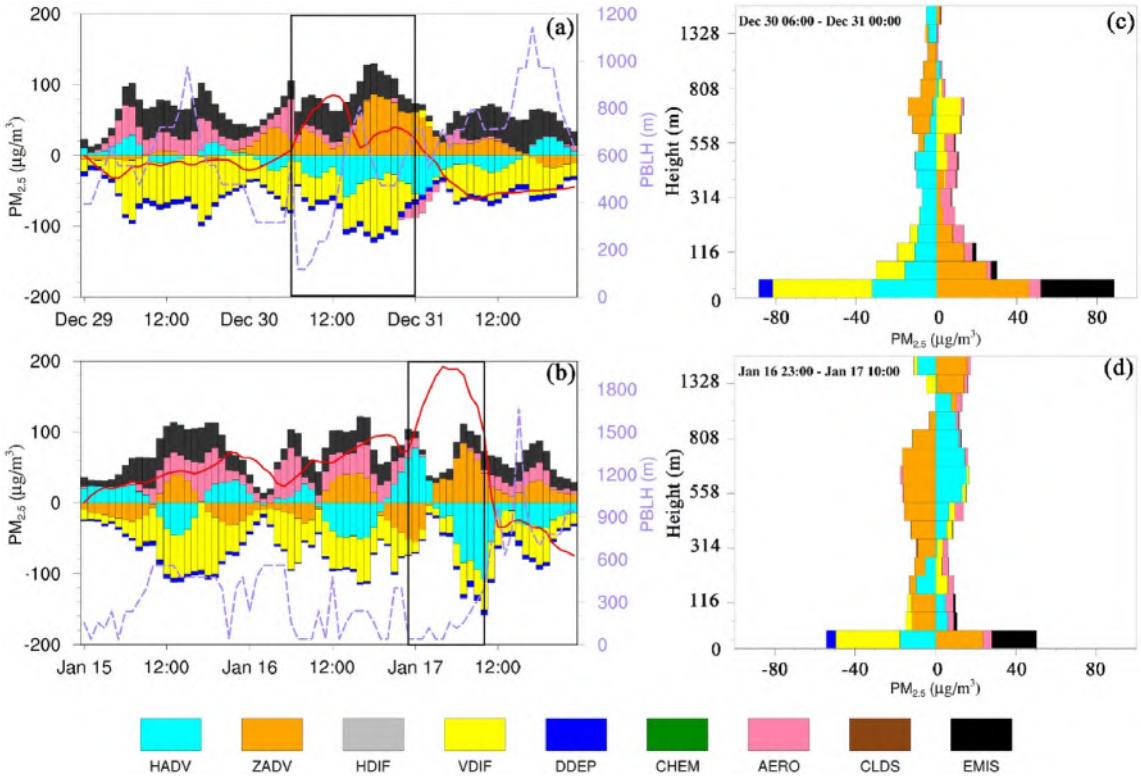

Fig. 3. Left column: The time evolution of near surface (first layer) $PM_{2.5}$ resulting from different processes (histogram), hourly accumulated net change of $PM_{2.5}$ (red line) as well as the PBL height (dashed purple line; right Y Axis) during two events, 29 to 31 December 2015 (a), 15 to 17 January 2016 (b). Right column: Processes contributing to the changes of peak-period ($PM_{2.5}$ in different layers during two events, 06:00 on 30 December to 00:00 on 31 December 2015 (c), 23:00 on 16 January to 10:00 on 17 January 2016 (d).

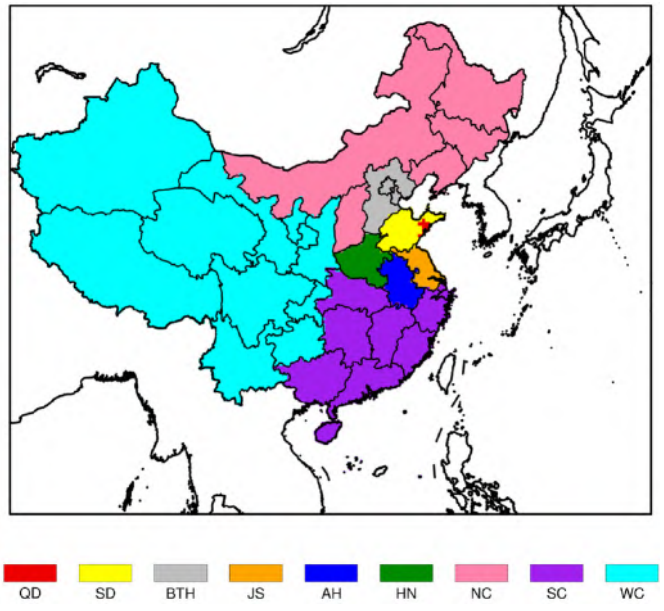

Fig. 4. Nine regions including Qingdao (QD), Shandong except Qingdao (SD), Beijing-Tianjin-Hebei (BTH), Jiangsu (JS), Anhui (AH), Henan (HN), other regions in Northern China (NC), Southern China (SC) and Western China (WC), with different colors marked for each region.

organic aerosol (SOA) were tagged and tracked separately.

During December 2015 and January 2016, the mean contribution from the local emissions in Qingdao is 25% (daily minimal/maximal contribution of 11%/50%) with the northern and western areas including SD, BTH, NC and WC accounting for 49% (results not shown), due to the dominant northwesterly wind direction. These results are comparable to the study by Li et al. (2017), who used HYSPLIT model and found that 44% of total air masses were derived from north and west regions and contributed to the $PM_{2.5}$ pollution in Qingdao during the similar period of winter 2015.

During the severe haze events, i.e., Event I, (29–31 December 2015), the three largest contributions come from QD (18%), SD (18%) and BTH (16%), respectively, with the total contribution of 52%. In particular, over the peak $PM_{2.5}$ period (from 06:00 on 30 December to 00:00 on 31 December; indicated by the black square in Fig. 5a), the contribution from BTH increased to 26%, illustrating the increased long-range transport impact from the northern area. Similar findings were reported by Chen et al. (2017), using CMAQ-ISAM to investigate the $PM_{2.5}$ pollution in Lingcheng located in the Shandong Province, where the contributions of the local emissions were found to be only 15.4% in 2013 and 2014, and the percentage was even smaller, with value of only 11.6%, on the heavy haze days (Table 5 of Chen et al. (2017)).

In comparison to Event I, some differences exist in Event II (from 15–17 January 2016). The three largest contributions over QD, SD and NC are 24%, 19% and 12%, respectively, with the dominant contribution from QD plus SD, accounting for 43% (Fig. 5b). The dominant contribution value becomes even larger during the $PM_{2.5}$ peak period (from 23:00 on 16 January to 10:00 on 17 January; indicated by the black square in Fig. 5b), i.e., 54% from QD plus SD. Thus, compared to Event I during which the contribution of QD, SD and BTH is comparable to each other, in Event II, the contributions of QD and SD is substantially larger than NC or BTH. To explain the differences and clearly examine the track of the sources, Lagrangian model WRF-FLEXPART will be applied and discussed below.

WRF-FLEXPART version 3.1 is employed to run 24-h backward

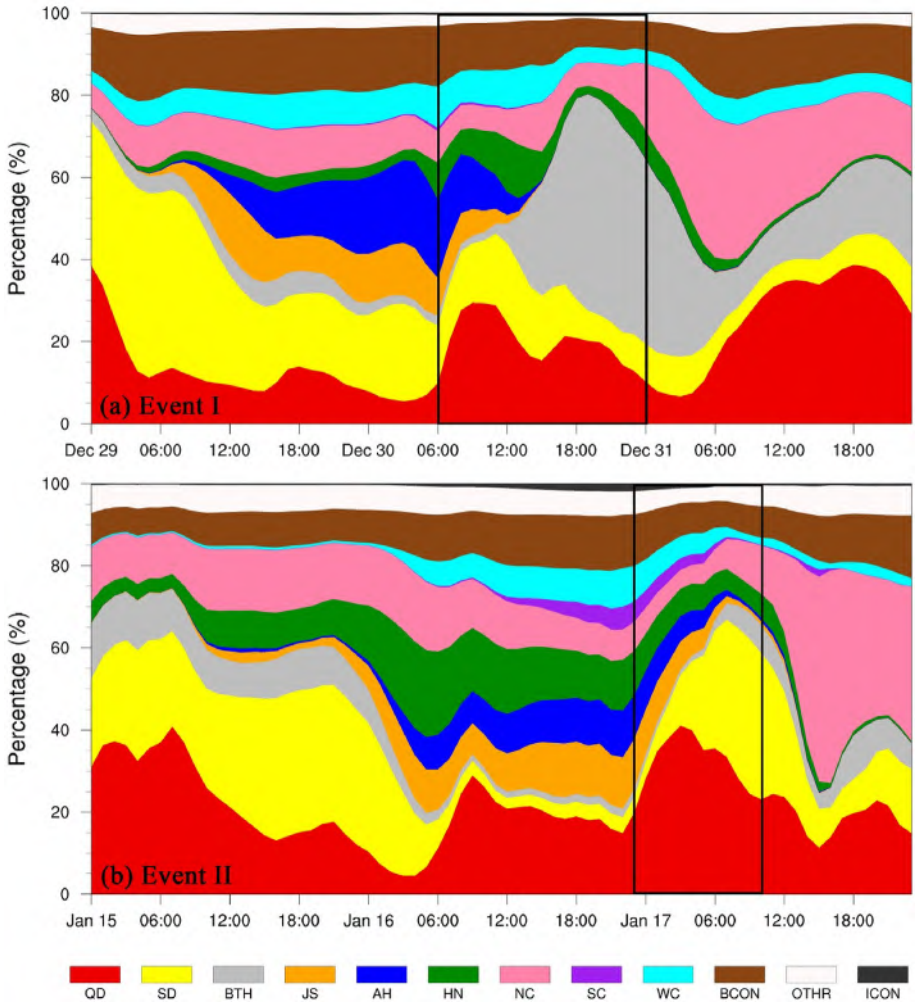

Fig. 5. The hourly percentage contribution of different regions to $PM_{2.5}$ concentration in Qingdao during Event I (29–31 December, 2015; Fig. 5a) and Event II (15–17 January, 2016; Fig. 5b). Region definitions were shown in Fig. 4.

trajectories five times each day, i.e., one trajectory every 6 h at local time 00:00, 06:00, 12:00, 18:00 and 24:00 during every event. The receptor location is at Qingdao (36.05–36.17°N, 120.30–120.50°E) with the altitude of 0–100 m above the ground level. For one trajectory, the total number of particles to be released is 1000. As verification, the trajectory produced by FLEXPART is used to compare with Hybrid Single Particle Lagrangian Integrated Trajectory model (HYSPLIT; https://ready.arl.noaa.gov/HYSPLIT_traj.php), mainly considering the meteorological conditions of HYSPLIT directly comes from the reanalysis data. The results from HYSPLIT are in general consistent with the results from WRF-FLEXPART, therefore, no results from HYSPLIT are shown here.

During Event I, the $PM_{2.5}$ in the first 30 h of Event I (from 00:00 on 29 December to 06:00 on 30 December) is mainly from Shandong (yellow shading in Fig. 5a) and those provinces south of QD (JS in orange, AH in blue and HN in green; region shown in Fig. 4). After 06:00 on 30 December 2015, PBL becomes substantially low (only 100-m or so; Fig. 3a), the $PM_{2.5}$ accumulation is sufficiently fast, with a peak value of 218 $\mu g/m^3$ at the hour of 12:00 on 30 December 2015 and the contributions from QD (red) plus SD (yellow) account for 44% (Fig. 5a). After 12:00 the wind direction gradually shifts from the south to the north (pink to yellow and purple colors in Fig. 6b), leading to the BTH dominating the transport and contribution (Fig. 5a).

In Event II, the backward trajectories on 15 January 2016 concentrated over QD and SD (Fig. 6d), consistently with the large contributions from QD plus SD (Fig. 5b). On 16 January 2016, as reflected by FLEXPART (Fig. 6e), source regions expend further south including JS, AH and HN. Between 06:00 and 12:00 on 17 January 2016 (Fig. 6e), the transmission direction shifts from the south to the north. Liaoning province (NC) stands out as the main source region. Overall, the back trajectories show consistent results with the CMAQ-ISAM, indicating that the transport direction of air pollutants may modulate the impacts from different regions even in a short event period such as 3-days.

5. Conclusions

The processes of $PM_{2.5}$ pollution in Qingdao are investigated in this study, primarily through the process analysis and air-mass-trajectory-based source apportionment. During December 2015 and January 2016, the mean contribution from the local emissions in Qingdao is 25%, implicative of the vital contribution from other sources, such as the long-range transport from BTH. Two three-day episodic events (29–31 December 2015; 15–17 January 2016) were selected to deeply analyze the sources of $PM_{2.5}$. During these two events, the three largest contributions come from QD (18%), SD (18%) and BTH (16%), and, QD (24%), SD (19%) and NC (12%),

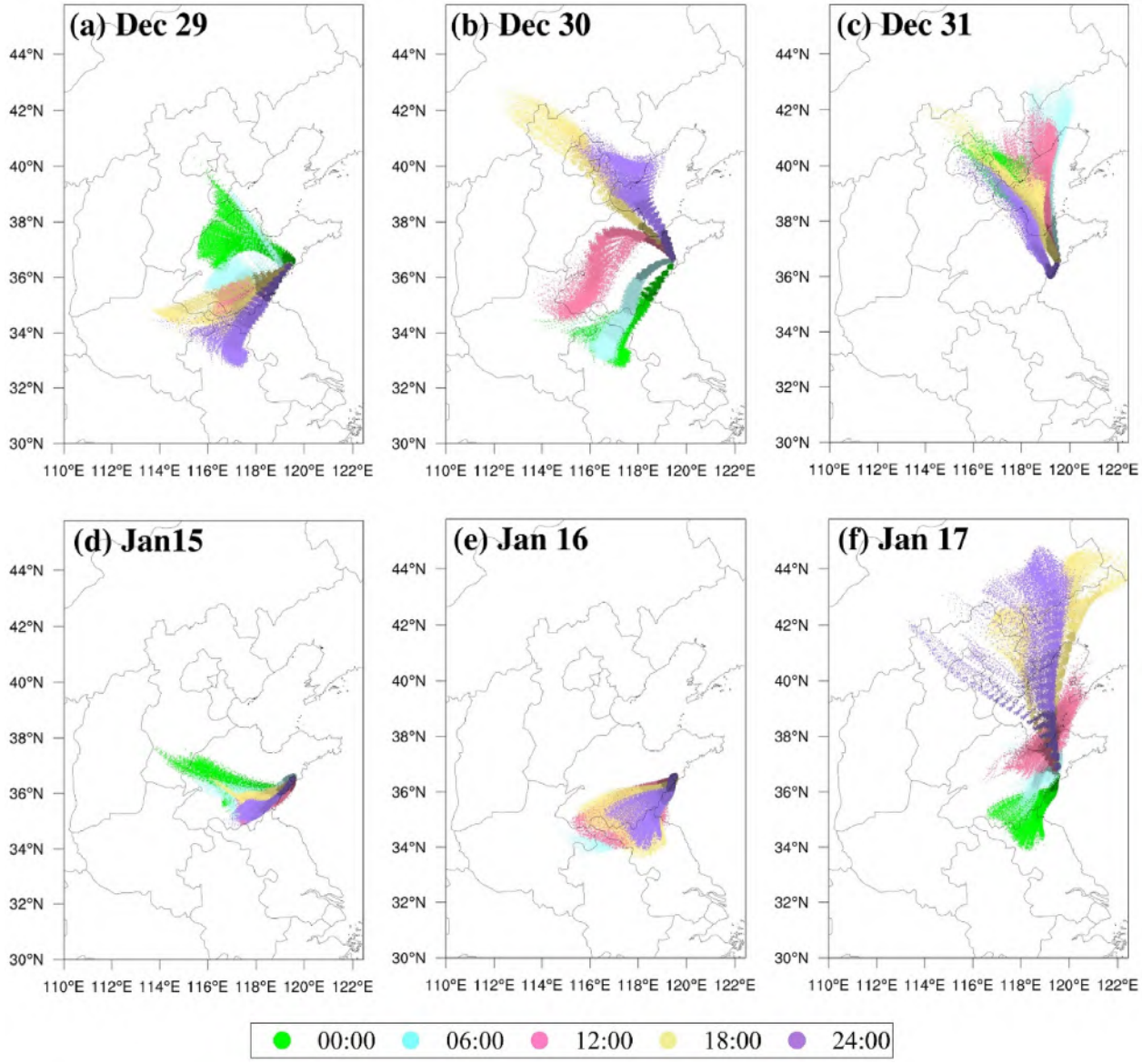

Fig. 6. The six-hourly transport pathways from WRF-FLEXPART from 29–31 December 2015, and 15–17 January 2016.

indicating that besides the significant contribution from local emission, the SD and northern areas such as BTH and NC play vital roles in affecting the air pollution in Qingdao. From the Lagrangian model FLEXPART, it shows the air pathways vary quickly in a daily or hourly scale, which thereby modulates the contribution of the source region, including both the magnitude and the location. Therefore, the $PM_{2.5}$ control strategy needs to be flexible to take this aspect into consideration.

Through the combination of WRF/CMAQ, CMAQ-ISAM as well as the WRF/FLEXPART, we not only can quantify the processes modulating the $PM_{2.5}$ in each hour, but also can easily track the air pathways. The results in general indicate that the transport and source apportionments follow the trajectories relatively well. However, the air trajectories can conveniently indicate the transport pathways. In particular, the track of air parcel is essential to verify the source contribution revealed by CMAQ-ISAM. Overall, this study paves the road that for future prediction or control policy in Qingdao, it is likely the Lagrangian model can more or less yield a good and quick estimation of the sources rather than the computational intensive three dimensional model such as CMAQ.

Declaration of competing interest

The authors declare that they have no conflict of interest.

CRediT authorship contribution statement

Yang Gao: Conceptualization, Methodology, Writing - original draft. **Huayao Shan:** Visualization, Formal analysis. **Shaoqing Zhang:** Writing - review & editing. **Lifang Sheng:** Writing - review & editing. **Jianping Li:** Writing - review & editing. **Junxi Zhang:** Visualization, Software. **Mingchen Ma:** Visualization, Software. **He Meng:** Validation. **Kun Luo:** Validation. **Huiwang Gao:** Writing - review & editing. **Xiaohong Yao:** Methodology, Writing - review & editing.

Acknowledgement

This research was supported by grants from the National Key Project of MOST (2017YFC1404101), National Natural Science Foundation of China (41776086), and Fundamental Research Funds for the Central Universities (201941006).

Appendix A. Supplementary data

Supplementary data to this article can be found online at https://doi.org/10.1016/j.chemosphere.2020.125861.

References

An, Z.S., Huang, R.J., Zhang, R.Y., Tie, X.X., Li, G.H., Cao, J.J., Zhou, W.J., Shi, Z.G., Han, Y.M., Gu, Z.L., Ji, Y.M., 2019. Severe haze in northern China: a synergy of anthropogenic emissions and atmospheric processes. Proc. Natl. Acad. Sci. U.S.A. 116, 8657–8666.

Brioude, J., Arnold, D., Stohl, A., Cassiani, M., Morton, D., Seibert, P., Angevine, W., Evan, S., Dingwell, A., Fast, J.D., Easter, R.C., Pisso, I., Burkhart, J., Wotawa, G., 2013. The Lagrangian particle dispersion model FLEXPART-WRF version 3.1. Geosci. Model Dev. 6, 1889–1904.

Byun, D., Schere, K.L., 2006. Review of the governing equations, computational algorithms, and other components of the models-3 Community Multiscale Air Quality (CMAQ) modeling system. Appl. Mech. Rev. 59, 51–77.

Cao, J.J., Lee, S.C., Chow, J.C., Watson, J.G., Ho, K.F., Zhang, R.J., Jin, Z.D., Shen, Z.X., Chen, G.C., Kang, Y.M., Zou, S.C., Zhang, L.Z., Qi, S.H., Dai, M.H., Cheng, Y., Hu, K., 2007. Spatial and seasonal distributions of carbonaceous aerosols over China. J. Geophys. Res. Atmos. 112, 9.

Cao, J.J., Shen, Z.X., Chow, J.C., Watson, J.G., Lee, S.C., Tie, X.X., Ho, K.F., Wang, G.H., Han, Y.M., 2012. Winter and summer $PM_{2.5}$ chemical compositions in fourteen Chinese cities. J. Air Waste Manag. Assoc. 62, 1214–1226.

Chan, C.K., Yao, X., 2008. Air pollution in mega cities in China. Atmos. Environ. 42, 1–42.

Chang, L.Y., Xu, J.M., Tie, X.X., Wu, J.B., 2016. Impact of the 2015 El Nino event on winter air quality in China. Sci. Rep. 6.

Chen, D., Liu, X., Lang, J., Zhou, Y., Wei, L., Wang, X., Guo, X., 2017. Estimating the contribution of regional transport to $PM_{2.5}$ air pollution in a rural area on the North China Plain. Sci. Total Environ. 583, 280–291.

Du, H., Li, J., Chen, X., Wang, Z., Sun, Y., Fu, P., Li, J., Gao, J., Wei, Y., 2019. Modeling of aerosol property evolution during winter haze episodes over a megacity cluster in northern China: roles of regional transport and heterogeneous reactions of SO_2. Atmos. Chem. Phys. 19, 9351–9370.

Duan, J., Huang, R.J., Lin, C.S., Dai, W.T., Wang, M., Gu, Y.F., Wang, Y., Zhong, H.B., Zheng, Y., Ni, H.Y., Dusek, U., Chen, Y., Li, Y.J., Chen, Q., Worsnop, D.R., O'Dowd, C.D., Cao, J.J., 2019. Distinctions in source regions and formation mechanisms of secondary aerosol in Beijing from summer to winter. Atmos. Chem. Phys. 19, 10319–10334.

Gao, H., Chen, J., Wang, B., Tan, S.-C., Lee, C.M., Yao, X., Yan, H., Shi, J., 2011. A study of air pollution of city clusters. Atmos. Environ. 45, 3069–3077.

Gao, Y., Fu, J.S., Drake, J.B., Lamarque, J.F., Liu, Y., 2013. The impact of emission and climate change on ozone in the United States under representative concentration pathways (RCPs). Atmos. Chem. Phys. 13, 9607–9621.

Huang, J., Pan, X., Guo, X., Li, G., 2018. Health impact of China's Air Pollution Prevention and Control Action Plan: an analysis of national air quality monitoring and mortality data. The Lancet. Planet. Health 2, e313–e323.

Ji, D., Li, L., Wang, Y., Zhang, J., Cheng, M., Sun, Y., Liu, Z., Wang, L., Tang, G., Hu, B., Chao, N., Wen, T., Miao, H., 2014. The heaviest particulate air-pollution episodes occurred in northern China in January, 2013: insights gained from observation. Atmos. Environ. 92, 546–556.

Khiem, M., Ooka, R., Hayami, H., Yoshikado, H., Huang, H., Kawamoto, Y., 2010. Process analysis of ozone formation under different weather conditions over the Kanto region of Japan using the MM5/CMAQ modelling system. Atmos. Environ. 44, 4463–4473.

Kwok, R.H.F., Napelenok, S.L., Baker, K.R., 2013. Implementation and evaluation of $PM_{2.5}$ source contribution analysis in a photochemical model. Atmos. Environ. 80, 398–407.

Li, L., Yan, D., Xu, S., Huang, M., Wang, X., Xie, S., 2017. Characteristics and source distribution of air pollution in winter in Qingdao, eastern China. Environ. Pollut. 224, 44–53.

Liu, T., Gong, S., He, J., Yu, M., Wang, Q., Li, H., Liu, W., Zhang, J., Li, L., Wang, X., Li, S., Lu, Y., Du, H., Wang, Y., Zhou, C., Liu, H., Zhao, Q., 2017. Attributions of meteorological and emission factors to the 2015 winter severe haze pollution episodes in China's Jing-Jin-Ji area. Atmos. Chem. Phys. 17, 2971–2980.

Ma, M., Gao, Y., Wang, Y., Zhang, S., Leung, L.R., Liu, C., Wang, S., Zhao, B., Chang, X., Su, H., Zhang, T., Sheng, L., Yao, X., Gao, H., 2019. Substantial ozone enhancement over the North China Plain from increased biogenic emissions due to heat waves and land cover in summer 2017. Atmos. Chem. Phys. 19, 12195–12207.

Miao, Y., Liu, S., Huang, S., 2019. Synoptic pattern and planetary boundary layer structure associated with aerosol pollution during winter in Beijing, China. Sci. Total Environ. 682, 464–474.

Skamarock, W.C., Klemp, J.B., Dudhia, J., Gill, D.O., Barker, D.M., Duda, M.G., Huang, X.-Y., Wang, W., Powers, J.G., 2008. A description of the advanced research WRF version 3, note, NCAR/TN-475CSTR. Natl. for Atmos. Res., Boulder, CO, USA available at: http://www2.mmm.ucar.edu/wrf/users/docs/arw_v3_bw.pdf.

Sun, Y., Chen, C., Zhang, Y., Xu, W., Zhou, L., Cheng, X., Zheng, H., Ji, D., Li, J., Tang, X., Fu, P., Wang, Z., 2016. Rapid formation and evolution of an extreme haze episode in Northern China during winter 2015. Sci. Rep. 6.

Teng, X., Hu, Q., Zhang, L., Qi, J., Shi, J., Xie, H., Gao, H., Yao, X., 2017. Identification of major sources of atmospheric NH_3 in an urban environment in northern China during wintertime. Environ. Sci. Technol. 51, 6839–6848.

Tian, M., Liu, Y., Yang, F., Zhang, L., Peng, C., Chen, Y., Shi, G., Wang, H., Luo, B., Jiang, C., Li, B., Takeda, N., Koizumi, K., 2019. Increasing importance of nitrate formation for heavy aerosol pollution in two megacities in Sichuan Basin, southwest China. Environ. Pollut. 250, 898–905.

US-EPA, 2007. Guidance on the Use of Models and Other Analyses for Demonstrating Attainment of Air Quality Goals for Ozone, $PM_{2.5}$, and Regional Haze. EPA -454/B-407-002.

Wang, Y., Wang, J., Zhang, M., Shi, L., 2019. Spatial correlation analysis of energy consumption and air pollution in beijing-tianjin-hebei region. In: Yan, J., Yang, H.X., Li, H., Chen, X. (Eds.), Innovative Solutions for Energy Transitions, pp. 4280–4285.

Wong, D.C., Yang, C.E., Fu, J.S., Wong, K., Gao, Y., 2015. An approach to enhance pnetCDF performance in environmental modeling applications. Geosci. Model Dev. 8, 1033–1046.

Wu, R.D., Zhou, X.H., Wang, L.P., Wang, Z., Zhou, Y., Zhang, J.Z., Wang, W.X., 2017. $PM_{2.5}$ characteristics in Qingdao and across coastal cities in China. Atmosphere 8, 19.

Xu, H., Bi, X.H., Zheng, W.W., Wu, J.H., Feng, Y.C., 2015. Particulate matter mass and chemical component concentrations over four Chinese cities along the western Pacific coast. Environ. Sci. Pollut. Res. Int. 22, 1940–1953.

Xu, Q., Wang, S., Jiang, J., Bhattarai, N., Li, X., Chang, X., Qiu, X., Zheng, M., Hua, Y., Hao, J., 2019. Nitrate dominates the chemical composition of PM2.5 during haze event in Beijing, China. Sci. Total Environ. 689, 1293–1303.

Zhang, G., Gao, Y., Cai, W., Leung, L.R., Wang, S., Zhao, B., Wang, M., Shan, H., Yao, X., Gao, H., 2019a. Seesaw haze pollution in North China modulated by the subseasonal variability of atmospheric circulation. Atmos. Chem. Phys. 19, 565–576.

Zhang, J., Gao, Y., Leung, L., Luo, K., Liu, H., Lamarque, J.-F., Fan, J., Yao, X., Gao, H., 2019b. Impacts of climate change and emissions on atmospheric oxidized nitrogen deposition over East Asia. Atmos. Chem. Phys. 19, 887–900.

Zhang, Q., Xue, D., Liu, X., Gong, X., Gao, H., 2019c. Process analysis of $PM_{2.5}$ pollution events in a coastal city of China using CMAQ. J. Environ. Sci. China 79, 225–238.

Zhang, Q., Xue, D., Liu, X., Gong, X., Gao, H., 2019d. Process analysis of $PM_{2.5}$ pollution events in a coastal city of China using CMAQ. J. Environ. Sci. (China) 79, 225–238.

Zhang, Q., Xue, D., Wang, S., Wang, L., Wang, J., Ma, Y., Liu, X.-H., 2017. Analysis on the evolution of PM2.5 heavy air pollution process in Qingdao. China Environ. Sci. 37, 3623–3635.

Zhang, Y., Ding, A., Mao, H., Nie, W., Zhou, D., Liu, L., Huang, X., Fu, C., 2016. Impact of synoptic weather patterns and inter-decadal climate variability on air quality in the North China Plain during 1980-2013. Atmos. Environ. 124, 119–128.